Full-Wave Analysis of Guiding Structures Using a 2-D Array of 3-D TLM Nodes

Hang Jin, *Member, IEEE,* and Rüdiger Vahldieck, *Senior Member, IEEE*

***Abstract*—This paper introduces a novel TLM approach to the full-wave analysis of guided wave structures. Instead of using real pulses as in the conventional TLM method, complex pulses are used in this new approach. Therefore a non-reciprocal phase shift in z-direction can be introduced which can be used to connect the z-arms in a 3-D node directly. As a result, the 3-D array of 3-D nodes, normally required in the TLM method to calculate the propagation and attenuation constant, is reduced to only one mesh unit in z-direction (2-D array of 3-D nodes). The propagation constant is determined by chosing a value and then calculating the frequency at which this value is valid from the Fourier Transform of the impulse response. Losses are found by computing the exponential decay of time harmonic solutions at the eigenfrequencies of the structure.**

I. Introduction

THE TRANSMISSION line matrix (TLM) method is a universal space-time domain technique first described by Johns and Beurle in 1971 [1]. Since then, several improvements have been made by various authors to enhance its efficiency [2]–[13]. Among them, Hoefer (i.e., [8]–[12]) has contributed significantly to develop the TLM method to what it is today: a very attractive and flexible numerical tool to analyze arbitrary electromagnetic field problems. As a result, the TLM method has received increased recognition in recent years as a useful numerical tool for the full-wave analysis of arbitrarily shaped (optical and microwave) guiding structures [8], [9], [13]. The basic steps in developing the method involves resonating a section of the guiding structure by placing shorted planes along the axis of propagation. The distance L between the shorted planes then equals a quarter of the guided wavelength of the mode at a frequency which is determined by the resonant frequency of the cavity. By changing the distance L, which changes the phase constant $\beta = \pi/2L$, and repeating the calculation of the resonant frequency of the cavity for each β, the dispersion characteristic of a particular structure can be obtained. This conventional TLM approach employs a three-dimensional (3-D) mesh. The memory space and CPU-time required often become excessive, in particular for large and complicated structures where a fine mesh is necessary. Furthermore, for most design problems most of the information contained in the time-domain response is useless. For example, if only the propagation constant of the fundamental mode within a small frequency range of interest, there is no way in the conventional TLM method to exclude the rest of the mode spectrum, which is inherently involved in the time-domain response, at the beginning of the computation. This unwanted frequency information is carried through the calculation as "computational overhead." Therefore, for problems, where there is no need for the time-domain response, the TLM method was traditionally at a disadvantage over frequency-domain methods. On the other hand, the flexibility of the TLM method and its suitability for contour-driven software, which does not require rewriting the code when the boundary conditions change, make this method an attractive CAD tool.

To overcome the aforementioned problem and at the same time retain the flexibility of the TLM method to analyze arbitrarily shaped transmission line cross-sections, this paper introduces a new concept for the TLM full-wave analysis. This concept is based on the excitation of the TLM mesh by complex pulses rather than real pulses. By doing so, a non-reciprocal phase shift in the z-direction can be introduced to connect the z-arms in a 3-D node directly. As a result, the 3-D array of 3-D nodes, normally required in the TLM method to calculate the propagation and attenuation constant, can be reduced to only one mesh unit in z-direction, or a 2-D array of 3-D nodes. The propagation constant β is now chosen and the corresponding frequency is determined from the Fourier Transform of the impulse response. Although this approach provides only frequency selective information, this is in most circuit design or analysis problems all that is required. Compared to the conventional TLM approach applied to characterizing dispersive transmission lines, this new method is computationally significantly more efficient.

To explain the principle procedure of this new method, the organization of this paper is as follows. Section II introduces the theoretical steps and describes the implementation of this new approach into the TLM analysis. Section III presents the detailed steps leading to the computation of the dispersive propagation and attenuation characteristics for abitrarily shaped guiding structures. To illustrate the validity of this new approach, Section IV discusses numerical results for a variety of homogeneous and inhomogeneous transmission lines on lossy dielectric substrate and with lossy conductors of finite metallization thickness. The conclusion is presented in Section V.

II. Theory

The TLM method models the electromagnetic field problem by simulating the guided structure though a three-dimensional transmission line mesh as shown in Fig. 1. By scattering

Manuscript received December 26, 1991; revised July 21, 1992.

The authors are with the Department of Electrical and Computer Engineering, University of Victoria, P.O. Box 3055, Victoria, BC, Canada, VPW 3P6.

IEEE Log Number 9205460.

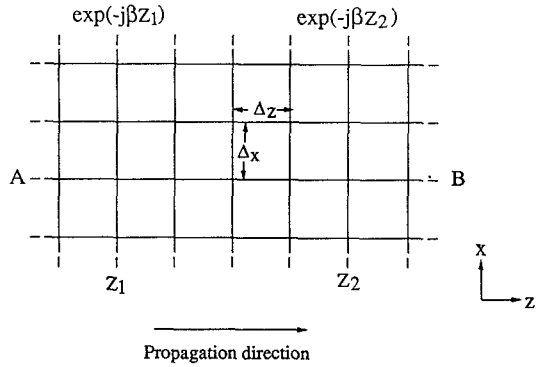

Fig. 1. The transmission line matrix in xz plane and the z-axis dependence of the modal field in a guiding structure.

impulses away from the transmission line junction (node) and then transfering the input from one node to the next in a fixed time step Δt, the problem becomes discrete in both space and time. This procedure can be described by a scattering event $\boldsymbol{S}$ relating incident impulses to reflected impulses at the time step $k\Delta t$ at each node:

$$ {}_k\boldsymbol{V}^r = \boldsymbol{S} \cdot {}_k\boldsymbol{V}^i \tag{1} $$

Then a transfering event $\boldsymbol{C}$, which relates reflected impulses to incident impulses in the adjacent node at the next time step $(k+1)\Delta t$, yields:

$$ {}_{k+1}\boldsymbol{V}^i = \boldsymbol{C} \cdot {}_k\boldsymbol{V}^r \tag{2} $$

$\boldsymbol{V}^i, \boldsymbol{V}^r$ are, respectively, vectors containing incident and reflected voltage impulses at each node. $\boldsymbol{S}$ and $\boldsymbol{C}$ are the scattering and connection matrices. The solution procedure can be initialized by launching a primary impulse into one of the nodes. The output is taken at some point in the mesh. It consists of a series of impulses and contains the information of the structure analyzed. This is the general solution procedure for the TLM method for arbitrary electromagnetic field problems.

To appreciate the modifications made in this paper one must recall that a guiding structure is characterized by propagating modes which are described by $\exp(-j\beta z)$, where β is the propagation constant. Hence, for a specific mode, the fields at plane $z = z_1$ and $z = z_2$ for example (Fig. 1), have only a phase difference of $\beta(z_2 - z_1)$. This *a priori* knowledge of the z-dependence of the modal fields in the guiding structure can be used to simplify the solution procedure of the TLM method. Suppose one excites the mesh of Fig. 1 by launching impulses at the nodes along line A-B in axial z-direction with a step phase difference of $\beta\Delta_z$ for adjacent nodes, with Δ_z being the size parameter in axial direction of the mesh. These phase relations among the initial impulses will also hold for successive impulses at other nodes along the axial z direction as long as the guiding structure does not change along the propagation path, i.e., the impulse scattering and connection matrices are identical for all the nodes along the line. The incident and reflected impulses at nodes $z = z_2$ equal the reflected and incident impulses at nodes $z = z_1$, except that there is a decrease of $\beta(z_2 - z_1)$ in the phase. Hence, the incident impulses of lines 9 and 8 at the node $z = z_2$ at the time $(k+1)\Delta t$, which are the reflected impulses on line 2 and 4 of the next node along the positive z-axis at the time $k\Delta t$, equal the reflected impulses on lines 2 and 4 of the node at $z = z_1$ at the time $k\Delta t$, except that there is a decrease of $\beta(z_2 - z_1)$ in the phase. Similarly, the incident impulses at the node $z = z_1$ on lines 2 and 4 at time $(k+1)\Delta t$, which are the reflected impulses on lines 9 and 8 of the next node along the negative z direction at the time $k\Delta t$, equal the reflected impulses on line 9 and 8 of the node at $z = z_2$ at the time $k\Delta t$, except that there is an increase of $\beta(z_2 - z_1)$ in the phase. If the planes $z = z_1$ and $z = z_2$ are chosen so closely that only one node in z direction remains between them (that is $z_2 - z_1 = \Delta_z$), one can obtain the relation between the reflected voltage impulses of the node at the time $k\Delta t$ and the incident voltage impulses of the node at the time $(k+1)\Delta t$ on the line in z direction (Fig. 2):

$$ \begin{aligned} {}_{k+1}V_8^i &= \exp(-j\beta\Delta_z)\,{}_kV_4^r \\ {}_{k+1}V_9^i &= \exp(-j\beta\Delta_z)\,{}_kV_2^r \\ {}_{k+1}V_2^i &= \exp(+j\beta\Delta_z)\,{}_kV_9^r \\ {}_{k+1}V_4^i &= \exp(+j\beta\Delta_z)\,{}_kV_8^r \end{aligned} \tag{3} $$

where ${}_kV_4^r, {}_kV_2^r, {}_kV_9^r, {}_kV_8^r$ and ${}_{k+1}V_4^i, {}_{k+1}V_2^i, {}_{k+1}V_9^i, {}_{k+1}V_8^i$ are the reflected voltages at the time $k\Delta t$ and the incident voltages at time $(k+1)\Delta t$, respectively, on lines 4, 2, 9, 8.

At this point it should be emphasized that the novelty of this approach lies in the fact that the amplitudes of the impulses (V_n, (3)) are complex quantities and not real values as known from the conventional TLM method. The necessity of employing impulses with complex amplitudes is self-evident: impulses with real amplitudes can not satisfy (3). Physically, an impulse with a complex amplitude can also be interpreted as a pair of orthogonal real impulses, one for the real part and one for the imaginary part of the complex amplitude. Since the scattering and transmission matrices are real, there is no coupling between the real and the imaginary parts during scattering and propagation among the nodes. Coupling between them occurs only through (3). Hence, developing (3) with its real and imaginary part will result in eight real equations instead of four complex ones. By linearly combining two real solutions one obtains formally the same results as if one would use complex notation right from the start. The complex notation used in this paper does not change the TLM algorithm, but simplifies the formulation as well as the programming significantly.

Since the 3-D node is closed in axial direction as presented by (3), the iteration procedure for the impulse propagation and scattering in space needs only be carried out in x, y directions. This effectively reduces the computational domain a two-dimensional array of 3-D-nodes which significantly reduces the memory space and computation time required. In other words, the normally three-dimensional array of 3-D-nodes is now reduced to only one slice. Because two travelling waves in opposite direction (+z and $-$z) are injected simultaneously into each node forming a standing wave within this slice, it is also called the resonating slice. The propagation constant (β) is found by using the following procedure. First a propagation constant is chosen and then impulses are injected into some of the nodes. These impulses will then propagate

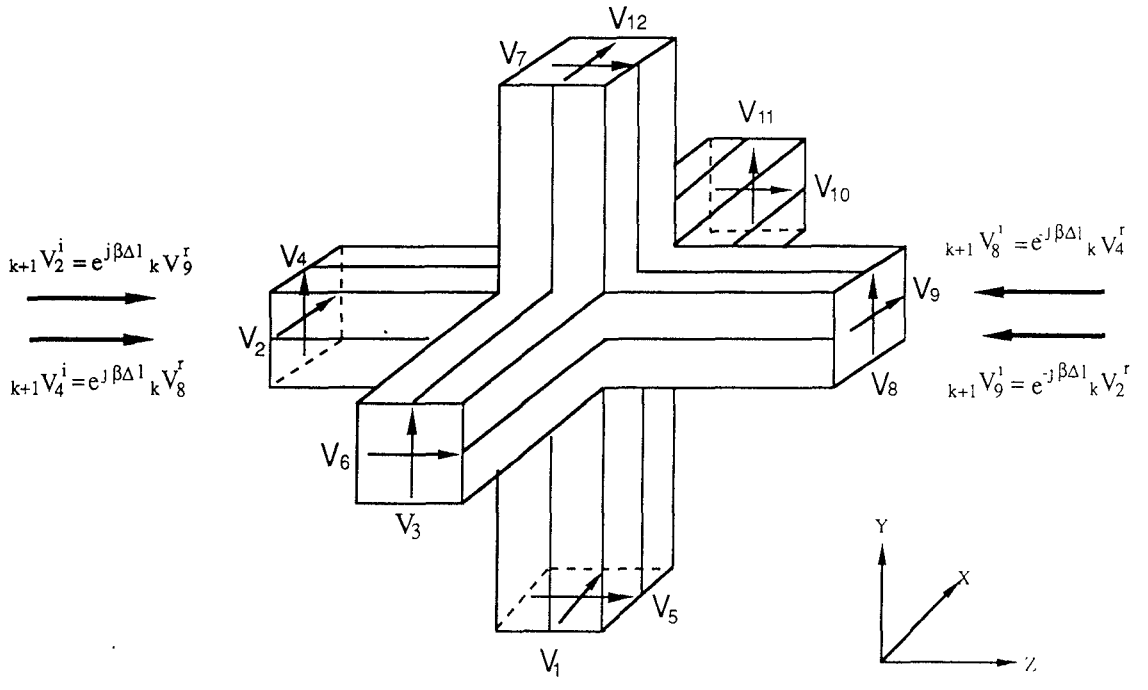

Fig. 2. The TLM node for all full wave analysis of a guiding structure.

and be scattered among the nodes. Those components of the electromagnetic fields corresponding to the modal fields of the guiding structure will be continually enhanced. After a sufficient number of iterations, the distributions of the impulses will correspond to the superposition of the modal fields. The output is taken at some nodes and consists of a series of impulses. Performing the Fourier transformation on those impluses, the peaks in the spectrum correspond to the resonant frequencies of the resonating slice for a given β. Thus a relationship is established between the propagation constant β and the frequency of the modes of the structure. Each β requires a separate TLM run. However, the topology of the TLM mesh for each of these runs need not be changed, because the propagation constant in the resonating slice is not related to the length Δz by $\beta = \pi/2\Delta_z$. Hence, different values of β can be computed with a fixed value of Δ_z. The conventional TLM method requires to change the length of the resonator for each value of β, which, in turn, requires to change the layout of the 3-D mesh.

III. Attenuation Coefficient

The computation of the attenuation coefficient for a lossy structure is more involved. In a lossy situation the fields will decay with time due to the absorption. For instance, at time $k\Delta t$, the electric field E^i of the ith mode can be written as:

$$E^i(k\Delta t) = E^i(0)\exp(j\omega_i k\Delta t)\exp\left(-\frac{\omega_i}{2Q_i}k\Delta t\right) \quad (4)$$

where ω_i is the resonance frequency for the ith mode which, for a given β, has been found by the previously described method. Q_i is the quality factor of the resonating slice. Since the fields calculated from the impulse distribution represent the total fields, which is the superposition of many modal fields, one needs to extract the component for the ith modal field. This can be accomplished by performing the Fourier transformation on the total fields at the resonant frequency ω_i as illustrated below:

$$\begin{aligned}\sum_{k=0}^{\infty} E(k\Delta t)\exp(-j\omega_i k\Delta t) &= \sum_{k=0}^{\infty} E^i(k\Delta t)\exp(-j\omega_i k\Delta t)\\ &= E^i(0)\sum_{k=0}^{\infty}\exp\left(-\frac{\omega_i}{2Q_i}k\Delta t\right)\\ &\approx E^i(0)\sum_{k=0}^{N}\exp\left(-\frac{\omega_i}{2Q_i}k\Delta t\right) \quad (5)\end{aligned}$$

Here $E(k\Delta t)$ is the total field at time $k\Delta t$ and N is an integer which is large enough to ensure the fields of all other modes, except the ith mode, will be cancelled out in (5). By choosing different values of N and making a curve fitting, the quality factor Q_i can be obtained from (5). The attenuation coefficient α for the lossy guiding structure is directly related to the quality factor Q of the resonator through the following relationship:

$$\alpha_i = \frac{\omega_i}{2Q_i V_{gi}} = \frac{\omega_i}{2Q_i}\frac{1}{\left(\frac{d\omega}{d\beta}\right)_i} \quad (6)$$

where b_{gi} is the group velocity of the ith mode.

IV. Numerical Results

Various calculations and comparisons have been made to validate this new approach. In the following computations, the 3-D hybrid symmetrical condensed node [14] is used.

The choice of the size parameters Δ_x, Δ_y in the x, y axes are dictated by the configuration of the guiding structure. In principle, the size parameter Δ_z in axial direction, which is the same for all the nodes of the mesh, can be chosen arbitrarily. It is found, however, that the value of Δ_z has a considerable effect on the convergence speed of the computation. The optimum value of Δ_z has not been found yet. In our calculations, Δ_z is set to be $(\Delta_l + \Delta_m)/2$, where Δ_l and Δ_m are the minimum and maximum values, respectively, of all the size parameters Δ_x, Δ_y in x, y directions throughout the mesh. The calculation of the attenuation coefficient α requires the mode group velocity V_{gi} (6) which is approximated by the following finite difference form:

$$V_{gi} = \left(\frac{d\omega}{d\beta}\right)_i \approx \frac{\Delta\omega_i}{\Delta\beta_i} \tag{7}$$

where $\Delta\beta_i$ is a small change of the propagation constant β_i and $\Delta\omega_i$ is the corresponding change of the resonant frequency of the resonating slice.

The first calculation is made for a rectangular waveguide filled with a lossy dielectric. Its cross section is divided into a uniform 8×4 mesh. The relative dielectric constant is $\varepsilon_r = 4$ and conductivity of the material $\sigma_d = 0.0001$ S/cm. The waveguide wall is assumed to be perfectly conducting. Calculations show that the resonant frequency ω converges much faster than the attenuation coefficient α for a given β. In the present case, it is found that the change of β is within 1% when the iteration number N is more than 500 while α reaches its stable value after $N = 1000$. This is possibly due to the fact that the resonant frequency for each mode is only determined by locating the corresponding peak position in the Fourier transformation spectrum of the output impulses while for the calculation of α the absolute value of the field is necessary. Also, only a one step calculation is required per β while α requires a two-step procedure. Fig. 3 shows the calculated results of β and α for the fundamental mode TE_{10} and the corresponding exact solutions. It is obvious that our calculated results are in good agreement with the exact ones.

A comparison with other methods is also made. Fig. 4 shows the TLM results of β and those of the mode matching method for a shield suspended coupled dielectric guide [15]. Also here the comparison is good. Fig. 5 shows the TLM results of β and α and those obtained from the finite element method for a shielded lossy image guide [16]. It is found that the TLM solutions are close to the FEM results.

Further calculations have been made for more complicated guiding structures. Fig. 6 shows results for a microstrip line with lossy conductor and groundplane, finite metallization thickness and lossy dielectric. Good agreement is found between experimental data [17], the mode matching technique [18] and the method presented in this paper. For the metal layer a selfconsistent approach is used, which means the metal is considered a dielectric with high conductivity. To incorporate the lossy groundplane into the TLM algorithm, the following complex boundary reflection coefficient is used:

$$\rho = \frac{Zc - Za}{Zc + Za} \tag{8}$$

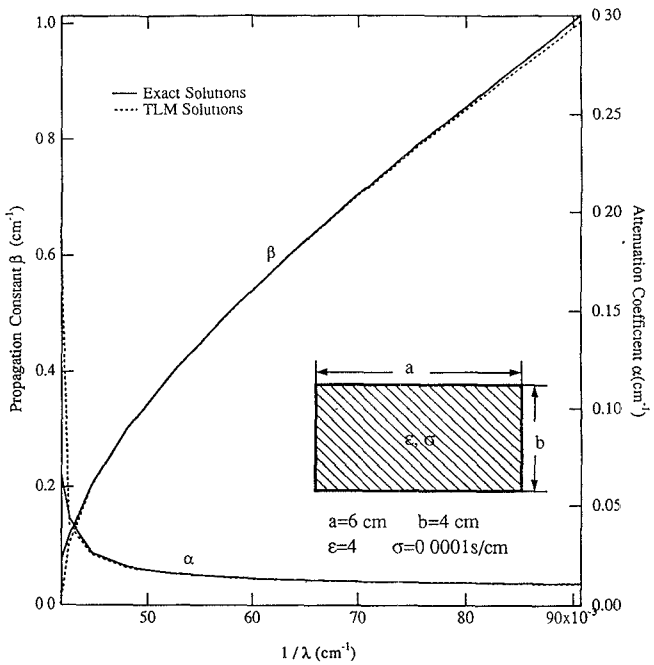

Fig. 3. Propagation constants and attenuation coefficients versus frequency for a rectangular waveguide filled with a lossy dielectric.

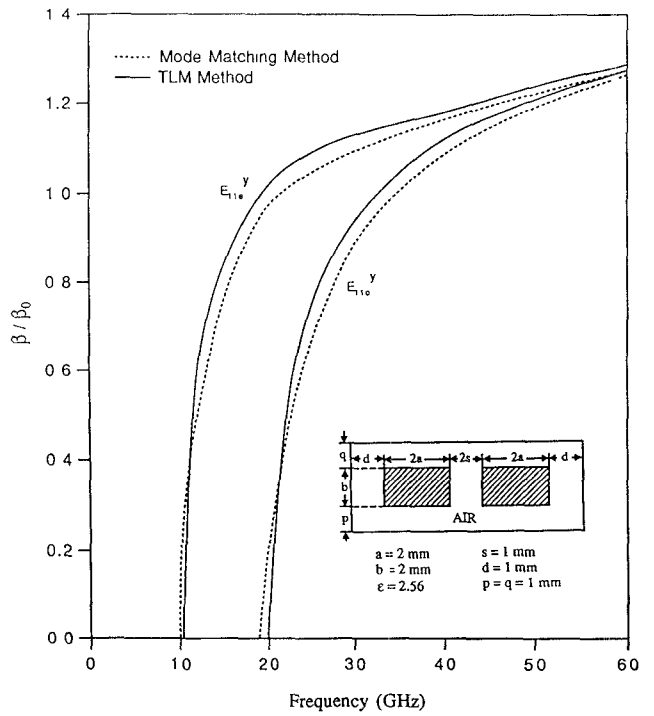

Fig. 4. Variation of β/β_0 versus frequency in a shielded suspended coupled dielectric guide.

where Zc is the wave impedance inside a perfect conductor

$$Zc = \sqrt{\frac{\mu\omega}{2\sigma}}(1 + j) \tag{9}$$

and Za is the characteristic impedance of the attached mesh lines. It should be noted, that since Zc depends on the frequency ω, the loss calculations for the lossy groundplane via the complex reflection coefficient needs two steps. For a given

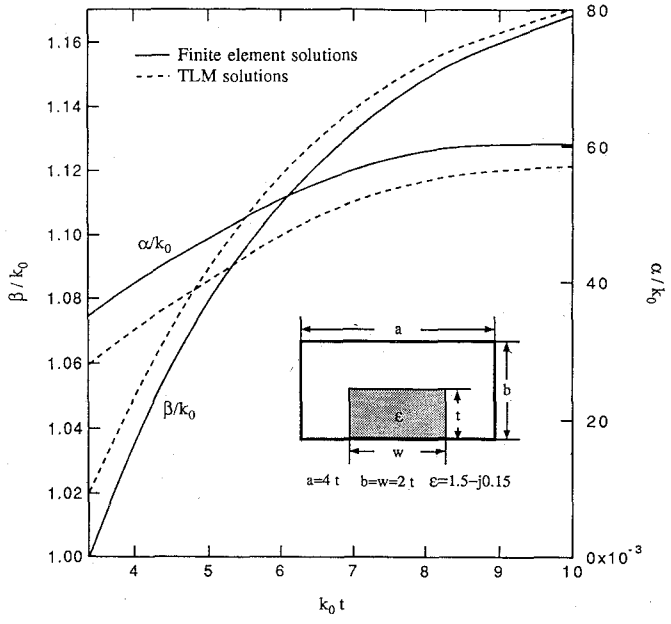

Fig. 5. Propagation constant and attenuation coefficients versus frequency for a shielded image guide composed of a lossy dielectric (E_{11}^y mode).

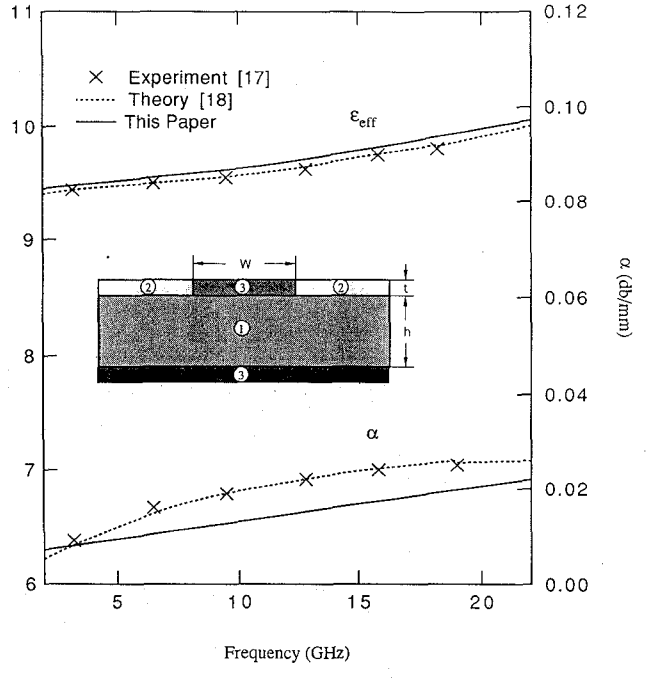

Fig. 6. Effective permittivities and attenuation coefficients versus frequency for a microstrip line with lossy conductor and groundplane, finite metallization thickness and lossy dielectric ($W = 0.55$ mm, $h = 0.2$ mm, $t = 0.006$ mm. The material parameters are: (1) GaAs: $\varepsilon_r = 12.9, \tan\delta = 3 \times 10^{-4}$; (2) Dielectric layer: $\varepsilon_r = 3.4, \tan\delta = 0.05$; (3) Strip and groundplane metallization: $\kappa = 17700$ s/mm.

β, a perfect conducting groundplane is assumed first and the resonant frequency ω is found. Then this ω is substituted into (9) as a first approximation from which the actual resonant frequency and the loss α will be determined. Comparing the shift in resonant frequency for the lossless and lossy case, it is found to be negligible. The total CPU-time per frequency sample on a SUN SPARC II station is less than 5 min. This is much less than what the conventional TLM algorithm would consume on the same serial machine. In comparison to other frequency-domain techniques, the computation time is smaller or comparable. However, considering that the method presented is capable of analyzing arbitrary transmission line cross-sections, including losses and finite metallization thickness, this method is far more flexible than most frequency-domain techniques and represents a very good compromise between flexibility and computational speed.

V. Conclusions

This paper presented a new concept for the TLM full-wave analysis of arbitrary guiding structure using a 2-D array of 3-D TLM nodes. In contrast to the conventional 2-D TLM approach, which can only be used to describe three components of the electromagnetic field, this new technique retains all the characteristics of the 3-D TLM method (necessary to describe six field components), but requires much less memory space and CPU-time. The basis for this new technique is that only one slice out of a 3-D mesh of 3-D TLM nodes is used. This slice can be viewed as a resonant section with dynamic boundaries. The propagation constant in this resonant section is chosen and the resonant frequency is determined by a Fourier transformation of the impulse response. This technique avoids changing the length of the resonator for each new β.

References

[1] P. B. Johns and R. L. Beurle, "Numerical solution of 2-dimensional scattering problems using a transmission-line matrix," *Proc. Inst. Elec. Eng.*, vol. 118, no. 9, pp. 1203–1208, Sept. 1971.

[2] P. Saguet and E. Pic, "Un traitement du signal simple four Ameliorer la Methode T.L.M.," *Electron. Lett.*, vol. 16, pp. 247–248, Mar. 1980.——, "Le maillage rectangulaire et le changement de Maillie dans la method TLM en deux dimensions," *Electron. Lett.*, vol. 17, pp. 277–279, April 1981.

[3] P. Johns, "A symmetrical condensed node for the TLM method," *IEEE Trans. Microwave Theory Tech.*, vol. MTT-35, pp. 370–377, Apr. 1987.

[4] R. H. Voelker and R. J. Lomax, "A finite-difference transmission line matrix method incorporating a nonlinear device model," *IEEE Trans. Microwave Theory Tech.*, vol. 38, pp. 302–312, Mar. 1990.

[5] P. Naylor and R. A. Desai, "New three dimensional symmetrical condensed lossy node for solution of electromagnetic wave problems by TLM," *Electron. Lett.*, vol. 26, pp. 492–494, Mar. 1990.

[6] F. J. German, G. K. Gothard, and L. S. Riggs, "Modelling of materials with electric and magnetic losses with the symmetrical condensed TLM method," *Electron. Lett.*, vol. 26, pp. 1307–1308, Aug. 1990.

[7] W. J. R. Hoefer, "The transmission-line matrix method - Theory and application," *IEEE Trans. Microwave Theory Tech.*, vol. MTT-33, pp. 882–893, Oct. 1985.

[8] ——, "The transmission line matrix (TLM) method," in *Numerical Techniques for Microwave and Millimeter-wave Passive Structure*, T. Itoh, Ed., New York: Wiley, 1989.

[9] P. P. M. So, Eswarappa and W. J. R. Hoefer, "A two-dimensional transmission line matrix microwave field simulator using new concepts and procedures," *IEEE Trans. Microwave Theory Tech.*, vol. MTT-37, pp. 1877–1884, Oct. 1989.

[10] Eswarrappa, G. I. Costache, and W. J. R. Hoefer, "Transmission line matrix modelling of dispersive wide-band absorbing boundaries with time-domain diakoptics for S-parameter extraction," *IEEE Trans. Microwave Theory Tech.*, vol. 38, pp. 379–386, Apr. 1990.

[11] Z. Chen, M. M. Ney, and W. J. R. Hoefer, "A new boundary description in two-dimensional TLM models of microwave circuits," *IEEE Trans. Microwave Theory Tech.*, vol. 39, pp. 377–382, Mar. 1991.

[12] G. E. Mariki and C. Yeh, "Dynamic three-dimensional TLM analysis of microstriplines on anisotropic substrate," *IEEE Trans. Microwave Theory Tech.*, vol. MTT-33, pp. 789–799, Sept. 1985.

[13] R. Scaramuzza and A. J. Lowery, "Hybrid symmetrical condensed node for the TLM method," *Electron. Lett.*, vol. 26, pp. 1947–1949, Nov. 1990.

[14] A. K. Tiwari, B. Bhat, and R. P. Singh, "Generalized coupled dielectric waveguide and its variants for millimeter-wave applications," *IEEE Trans. Microwave Theory Tech.*, vol. MTT-34, pp. 869–875, Aug. 1986.
[15] K. Hayata, K. Miura and M. Koshiba, "Finite-Element Formulation for Lossy Waveguides," *IEEE Trans. Microwave Theory Tech.*, vol. 36, pp. 268–276, Feb. 1988.
[16] H. J. Finlay, R. H. Jansen, J. A. Jenkins, and I. G. Eddison, "Accurate characterization and modeling of transmission lines for GaAs MMIC's," *IEEE Trans. Microwave Theory Tech.*, vol. 36, pp. 961–967, June 1988.
[17] W. Heinrich, "Full-wave analysis of conductor losses on MMIC transmission lines," *IEEE Trans. Microwave Theory Tech.*, vol. 38, pp. 1468–1472, Oct. 1990.

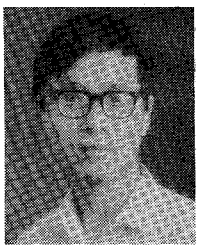

Hang Jin (M'91) was born in Jiangsu, China, on September 27, 1960. He received the B.Sc. degree in electrical engineering from the University of Science and Technology of China (USTC), Hefei, China, in 1982 and M.Eng. and D.Eng. degrees in electrical engineering from the University of Electronics Science and Technology of China, Chengdu, China, in 1984 and 1987, respectively.

Dr. Jin joined the Faculty at the University of Electronics Science and Technology of China in 1987 where he conducted research in the areas of electromagnetic scattering, radar absorbing material, and millimeter wave techniques. From 1989–1990, he was a postdoctoral fellow at the National Optics Institute, Quebec City, Canada. Since October 1990, he has been a Research Associate at the University of Victoria, Canada. His current research areas include numerical methods for 3-D electromagnetic field problems, CAD of microwave/millimeter wave integrated (monolithic) circuits, and planar and quasi-planar components for MMIC and MHMIC applications.

Rüdiger Vahldieck (M'85–SM'86), for a photograph and biography, see this issue, p. 430.